Supporting Information

Acid-triggering of light-induced charge-separation in hybrid organic/inorganic molecular photoactive dyads for harnessing solar energy

Elisabetta Benazzi,[a] Joshua Karlsson,[a] Youssef Ben M'Barek,[b] Pavel Chabera,[c] Sébastien Blanchard,[b] Sandra Alves,[b] Anna Proust,[b] Tönu Pullerits,[c] Guillaume Izzet[b],* Elizabeth A. Gibson.[a]*

[a] Energy Materials Laboratory, Chemistry: School of Natural and Environmental Science, Newcastle University, Newcastle upon Tyne, NE1 7RU, UK.

[b]Sorbonne Université, CNRS, Institut Parisien de Chimie Moléculaire, IPCM, 4 Place Jussieu, F-75005 Paris, France.

[c]Department of Chemical Physics and NanoLund, Lund University, Box 124, 22241, Lund, Sweden.

Methods

Triethylamine (TEA) was dried over CaH_2 and freshly distilled under argon before use. Dimethylformamide (DMF) was purchased stored under argon over molecular sieve. Other solvents and reagents were obtained from commercial sources and used as received. Reactions, unless otherwise mentioned, were carried out under dry argon by using standard Schlenk-tube techniques. 4,4-Difluoro-8-(4'-ethynylphenyl)-1,3,5,7-tetramethyl-2,6-diethyl-4-bora-3a,4a-diaza-s-indacene,[1] $\mathbf{K^{W}_{Sn}[I]}$,[2] $\mathbf{K^{Mo}_{Sn}[I]}$[3] and $[Pd(PPh_3)_2Cl_2]$[4] were synthesized according to literature procedures. Microwave assisted syntheses were performed at an ambient pressured reactor (Milestone Start S) equipped with a temperature control unit. Other solvents and reagents were obtained from commercial sources and used as received. The ^{1}H (300.3 MHz), $\{^{1}H\}$ ^{31}P (121.5 MHz) and ^{19}F (282.4 MHz) NMR spectra were obtained at room temperature in 5 mm o.d. tubes on a Bruker AvanceII 300 spectrometer equipped with a QNP probe head. IR spectra were recorded from KBr pellets on a Jasco FT/IR 4100 spectrometer. Electrochemical studies were performed on an Autolab PGSTAT 100 workstation. A standard three electrode cell was used, which consisted of a working vitrous carbon electrode, an auxiliary platinum electrode and an aqueous saturated calomel electrode (SCE) equipped with a double junction. Elemental analyses were performed at the Institut de Chimie des Substances Naturelles, Gif sur Yvette, France. UV-visible absorption spectra were recorded on a Shimadzu UV-1800 spectrophotometer. Photoluminescence spectroscopy measurements in solution were recorded using a Shimadzu RF-6000 spectrofluorophotometer. All measurements were performed using quartz cuvettes with a path length of 1 cm, and samples were dissolved in spectroscopic grade solvents. The emission spectra were collected from solutions of the same absorbance at the excitation wavelength and we compared the area under the emission curves to evaluate the relative quantum yield. Fluorescence quantum yields were evaluated against Rhodamine 6G (Sigma) in EtOH. The ESI mass spectra were recorded using an LTQ Orbitrap hybrid mass spectrometer (Thermofisher Scientific, Bremen, Germany) equipped with an external ESI source operated in the negative ion mode. Spray conditions included a spray voltage of 3 kV, a capillary temperature maintained at 280 °C, a capillary voltage of −30 V, and a tube lens offset of −90 V. Sample solutions in acetonitrile (10 $pmol.\mu L^{-1}$) were infused into the ESI source by using a syringe pump at a flow rate of 180 $\mu L.h^{-1}$. Mass spectra were acquired in the Orbitrap analyzer with a theoretical mass resolving power (R_p) of 100 000 at m/z 400, after ion accumulation to a target value of 10^5 and a m/z range from m/z 300 to 2000. All data were acquired using external calibration with a mixture of caffeine, MRFA peptide and Ultramark 1600 dissolved in Milli-Q

water/ HPLC grade acetonitrile (50/50, v/v). Elemental analyses were performed at the Institut de Chimie des Substances Naturelles, Gif sur Yvette, France.

Transient Absorption Spectroscopy

Transient absorption spectroscopy was performed on solution samples of the bodipy with an optical density 0.25 to 0.9, in a 1 mm pathlength quartz cuvette. The samples were purged with N_2 before each measurement. The transient absorption setup was based on an amplified Ti:sapphire laser (Mai-Tai, Spitfire; both Spectra Physics) providing 80 fs pulses at 800 nm at the rate of 1 kHz. The pulses were split into two beams: excitation pulses (525 nm) were generated by optical parametric amplifier OPA (TOPAS C), Light Conversion) and probe pulses (white light supercontinuum) were generated by a CaF_2 crystal. The excitation and delayed probe beams were set to overlap in the sample (1 mm quartz cuvette). Consequently, the probe beam was dispersed on a photodiode array coupled to a spectrograph (Pascher Instruments). The transient absorption signal was calculated from a difference between spectra of two consecutive probe pulses passing though excited and unexcited sample, respectively. This was maintained by an optical chopper running at a frequency of 500 Hz which was synchronized with the laser. The angle between polarizations of excitation and probe beam were set to the so-called magic angle (54.7 degrees) to avoid observation of dynamics connected to transition dipole rotation. The excitation intensity used (650 µW, corresponding to 1.3 nJ per pulse and a spot size of ~700 µm diameter (FWHM)) did not lead to any visible photodegradation of the samples over the measurement period. Nanosecond laser flash photolysis measurements on **K^{W}_{Sn}[BOD]** were performed with a commercial setup (Applied Photophysics LKS-70) where excitation was provided by a 4 ns pulsed laser at 532 nm, 80 mJ per pulse. For recording the ns-µs dynamics of **K^{Mo}_{Sn}[BOD]** an externally triggered Q-switched Nd: YVO_4 laser (Advanced Optical Technology, 532 nm, 1 ns pulses) was used as a pump source, while the ordinary femtosecond detection with supercontinuum probe was used to record the transient changes in the absorption. The experimental conditions were nearly identical as for the femtosecond measurements with excitation wavelength 532 nm and intensity of ~600 µW.

Global analysis was performed using the program OPTIMUS.[23] The chirp correction was applied prior to global analysis. In global lifetime analysis, a model function for each detection wavelength is constructed. The optimisation is initiated with some starting values used to calculate each of the basic functions. The amplitudes of each function are found by linear fitting using the Moore-Penrose pseudoinverse (MATLAB pinv function). The fit parameters are optimised iteratively to minimise the square of the residual norm. The amplitudes are plotted against the detection wavelength to yield the decay associated spectra. The evolution associated spectra were determined by solving a system of differential equations using a sequential relaxation scheme. The fit parameters are optimised iteratively to minimise the square of the residual norm. The amplitudes are plotted against the detection wavelength to yield the evolution associated spectra (EAS), which represent the stationary spectra of the model compartments. For the sequential relaxation scheme, the decay associated spectra (DAS) of the lifetime components was calculated from a linear combination of the EAS of the compartments.

Synthesis

Reactions, unless otherwise mentioned, were carried out under dry argon by using standard Schlenk-tube techniques.

Synthesis of **K^{W}_{Sn}[BOD]**:

A mixture of **K^{W}_{Sn}[I]** (200mg, 0.05 mmol, 1 equiv), 4,4-Difluoro-8-(4'-ethynylphenyl)-1,3,5,7-tetramethyl-2,6-diethyl-4-bora-3a,4a-diaza-s-indacene (41 mg, 0.1 mmol, 2 equiv), CuI (0.72 mg, 3.7×10^{-3} mmol, 0.1 equiv) and $[Pd(PPh_3)_2Cl_2]$ (1.4 mg, 2×10^{-3} mmol, 0.04 equiv) in 4 mL of dry DMF was prepared in a Schlenk tube under argon atmosphere. After careful degassing with argon for 10 minutes, freshly distilled TEA (60 mg, 0.6 mmol, 12 equiv) was added. The mixture was stirred at 70°C for 1 h, under microwave irradiation. The resulting dark red solution was precipitated with diethyl ether. The precipitate was filtered and dissolved with TBABr (300mg) in dichloromethane (40mL) then the mixture was stirred for 20min. The resulting solution was

extracted three times with water (3x40mL). The resulting organic phase was then filtered on a cellulose membrane and precipitated using EtOH (40mL). After centrifugation, the supernatant was removed and the resulting solid washed with Et_2O yielding a bright pink powder (145 mg, Yield: 68%). ^{1}H NMR (CD_3CN): δ (ppm) 7.76 (d+dd, J_{HH} = 8.1 Hz, J_{SnH} = 95 Hz, 2H), 7.74 (d, J = 8.4 Hz, 2H), 7.67 (d+dd, J_{HH}=8.1, J_{SnH}= 34 Hz, 2H), 7.38 (d, J = 8.4 Hz, 2H), 3.11 (m, 32H), 2.48 (s, 6H), 2.35 (q, J = 7.4 Hz, 4H), 1.62 (m, 32H), 1.39 (h, J = 7.4 Hz, 32H), 1.37 (s, 6H), 0,98 (t, J = 7.4 Hz, 54 H); ^{31}P (CD_3CN): δ (ppm) -11.04 (s+d, J_{SnP} = 24 Hz); ^{19}F (CD_3CN): δ (ppm) -145.07 (q, J_{BF} = 33 Hz); ^{11}B (CD_3CN): δ (ppm) 1.68 (t, J_{BF} = 33 Hz). IR (KBr pellet, cm^{-1}): ν (cm^{-1}) 2960 (s), 2871 (s), 2360 (w),1653 (w), 1541 (m), 1479 (m), 1320 (m), 1195 (s), 1062 (s), 1035 (s), 943 (s), 867 (s), 787 (s). Elemental analysis for $PW_{11}O_{39}SnC_{95}H_{174}N_6BF_2$ (%): calcd C 26.88; H 4.13; N 1.98; found C; 27.08 H 4,11; N. 2.23.

Synthesis of **K^{Mo}_{Sn}[BOD]**:

A mixture of **K^{Mo}_{Sn}[I]** (200mg, 0.067 mmol), 4,4-Difluoro-8-(4'-ethynylphenyl)-1,3,5,7-tetramethyl-2,6-diethyl-4-bora-3a,4a-diaza-s-indacene, CuI (1.5 mg, 7.9×10-3 mmol, 0.1 equiv) and $[Pd(PPh3)_2Cl_2]$ (3.7 mg, 8×10^{-3} mmol, 0.08 equiv) in 4 mL of dry DMF was prepared in a Schlenk tube under argon atmosphere. After careful degassing with argon for 10 minutes, freshly distilled TEA (67 mg, 0.67 mmol, 10 equiv) was added. The mixture was stirred at 70°C for 1 h, under microwave irradiation. The resulting dark red solution was precipitated with diethyl ether. The precipitate was filtered and dissolved with TBABr (300mg) in dichloromethane (40mL) then the mixture was stirred for 20min. The resulting solution was extracted three times with water (3x40mL). The resulting organic phase was then filtered on a cellulose membrane and precipitated using EtOH (40mL). After centrifugation, the supernatant was removed and the resulting solid washed with Et_2O yielding a dark purple solid (105 mg, Yield: 48%). ^{1}H NMR (CD_3CN): δ (ppm) 7.72 (d+dd, J_{HH} = 7.8 Hz, J_{SnH} = 94 Hz, 2H), 7.71 (d, J = 8.1 Hz, 2H), 7.62 (d+dd, J_{HH}=7.8, J_{SnH}= 34 Hz, 2H), 7.38 (d, J = 8.1 Hz, 2H), 3.13 (m, 32H), 2.48 (s, 6H), 2.34 (q, J = 7.4 Hz, 4H), 1.63 (m, 32H), 1.40 (m, 32H), 1.37 (s, 6H), 0,98 (t, J = 7.1 Hz, 54 H); ^{31}P (CD_3CN): δ (ppm) -2.44 (s+d, J_{SnP} = 37Hz); ^{19}F (CD_3CN): δ (ppm) -145.07 (q, J_{BF} = 33 Hz); ^{11}B (CD_3CN): δ (ppm) 1.68 (t, J_{BF} = 33 Hz). IR (KBr pellet, cm^{-1}): ν (cm^{-1}) 2962 (s), 2873 (m), 2360 (w), 1653 (w), 1541 (m), 1479 (m), 1321 (m), 1195 (s), 1069 (s), 963 (s), 886 (s), 814 (s). Elemental analysis for $PMo_{11}O_{39}SnC_{95}H_{174}N_6BF_2.H_2O$ (%): calcd C 34.61; H 5.38; N 2.55; found C; 34.23 H 5.52; N. 2.34.

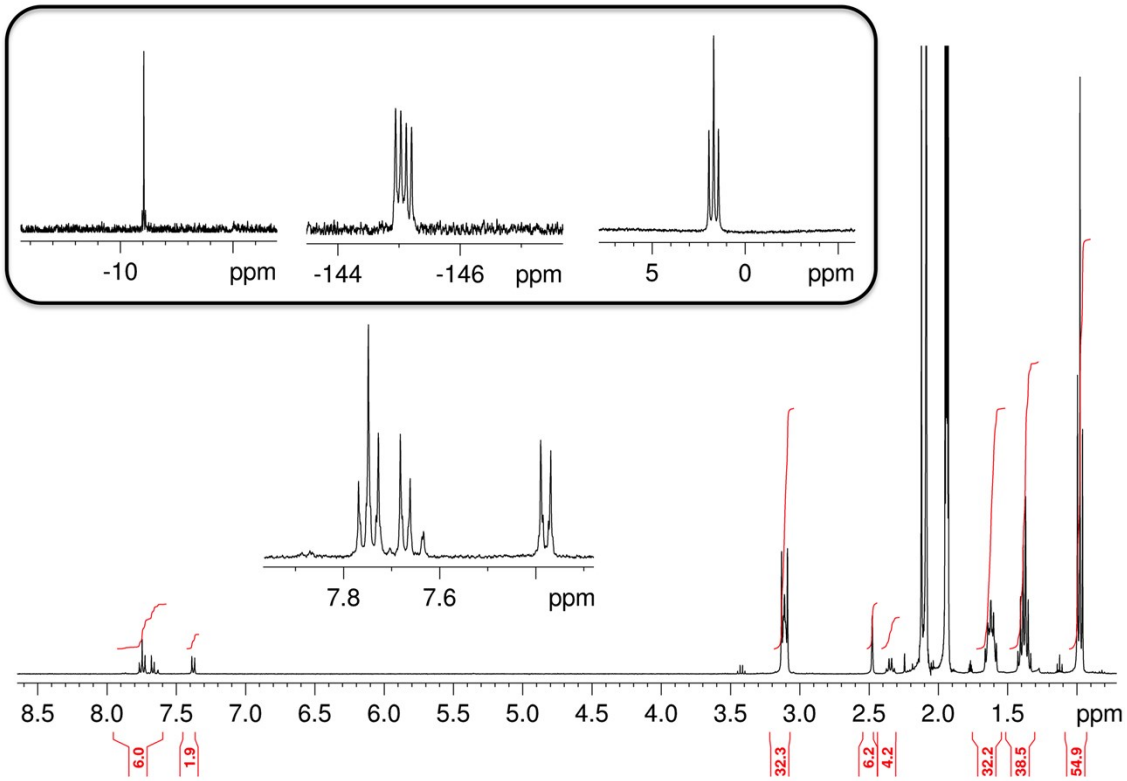

Figure S1. ^{1}H NMR (400 MHz) ^{31}P, ^{11}B and ^{19}F NMR (162, 128 and 376 MHz respectively, framed inset) spectra

of **K^{W}_{Sn}[BOD]** in CD_3CN.

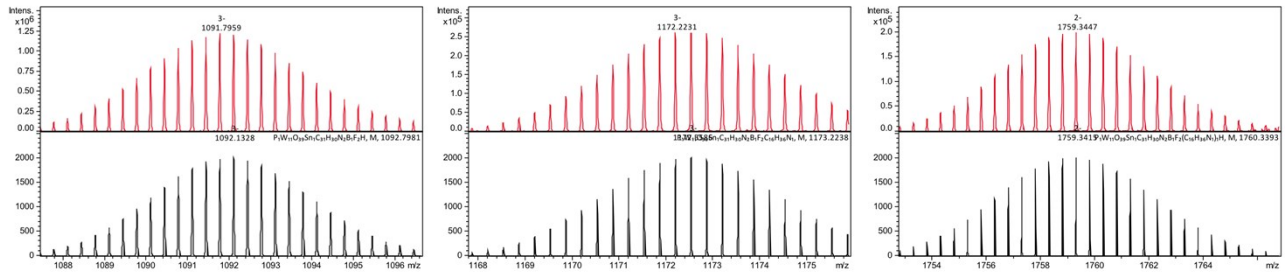

Figure S2. Comparison of experimental (upper trace) and calculated (lower trace) isotopic peaks for the ions $[PW_{11}O_{39}SnC_{31}H_{30}BF_2N_2.H]^{3-}$ (left), $[PW_{11}O_{39}SnC_{31}H_{30}BF_2N_2.TBA]^{3-}$ (middle) and $[PW_{11}O_{39}SnC_{31}H_{30}BF_2N_2.TBA.H]^{2-}$ (right) of **K^{W}_{Sn}[BOD]**.

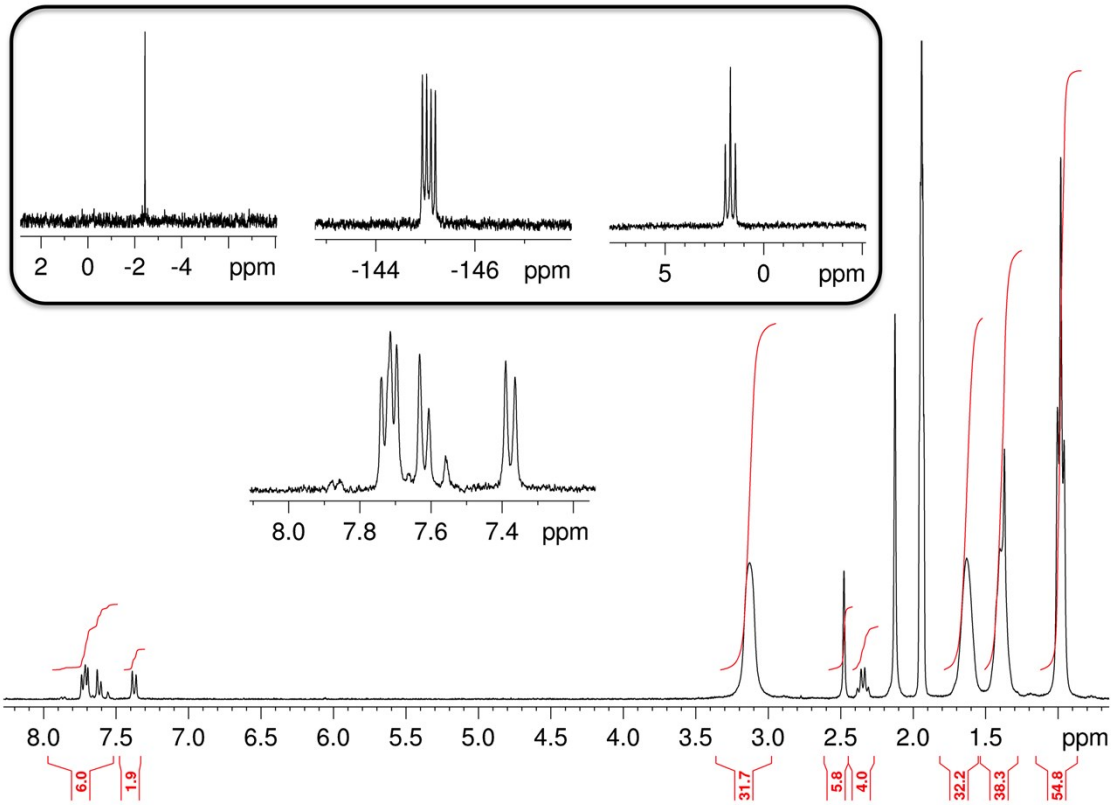

Figure S3. ^{1}H NMR (300 MHz) ^{31}P, ^{11}B, ^{19}F NMR and ^{19}F NMR (162, 128 and 376 MHz respectively, framed inset) spectra of **K^{Mo}_{Sn}[BOD]** in CD_3CN.

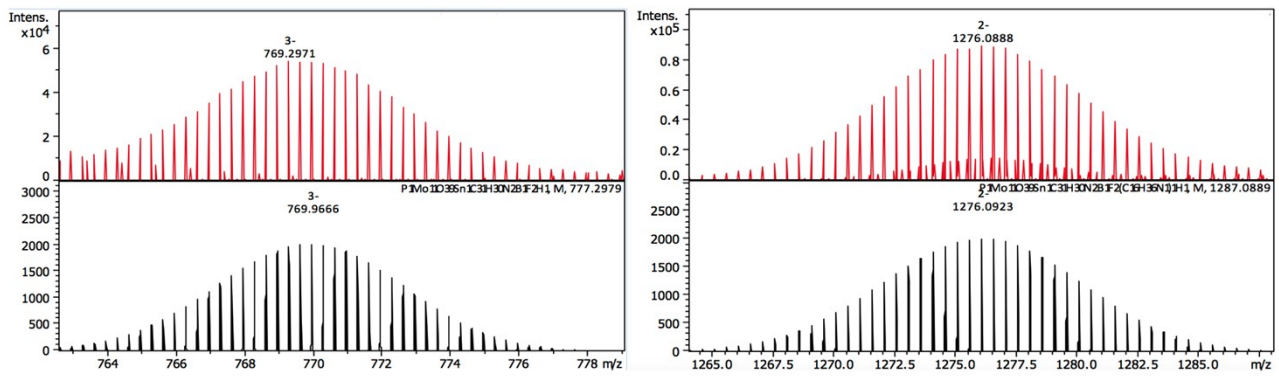

Figure S4. Comparison of experimental (upper trace) and calculated (lower trace) isotopic peaks for the ions $[PMo_{11}O_{39}SnC_{31}H_{30}BF_2N_2.H]^{3-}$ (left) and $[PMo_{11}O_{39}SnC_{31}H_{30}BF_2N_2.TBA.H]^{2-}$ (right) of **K^{Mo}_{Sn}[BOD]** (note that the minor isotopic peaks correspond to the aggregate $[(PMo_{11}O_{39}SnC_{31}H_{30}BF_2N_2)_2.TBA_2.H_3]^{3-}$).

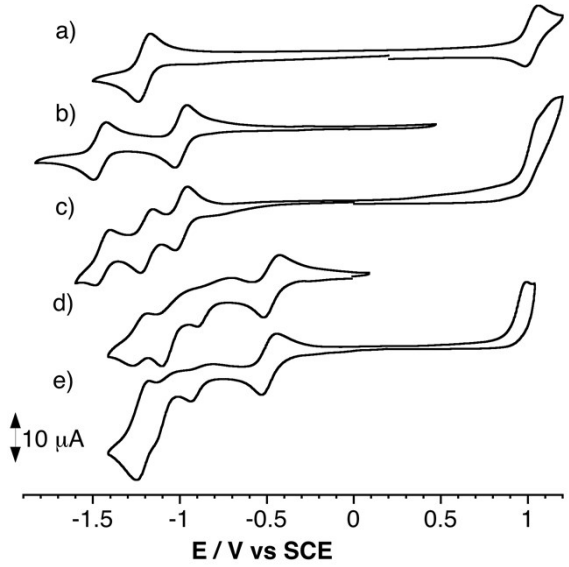

Figure S5. Cyclic voltammograms of *ca.* 1 mM solutions of reported compounds in MeCN containing 0.1 M of $TBAPF_6$: a) BOD-TMS, b) **K^{W}_{Sn}[I]**, c) **K^{W}_{Sn}[BOD]**, d) **K^{Mo}_{Sn}[I]**, e) **K^{Mo}_{Sn}[BOD]**. Scan rate, 20 mV s^{-1}; working electrode, glassy carbon; reference electrode, SCE.

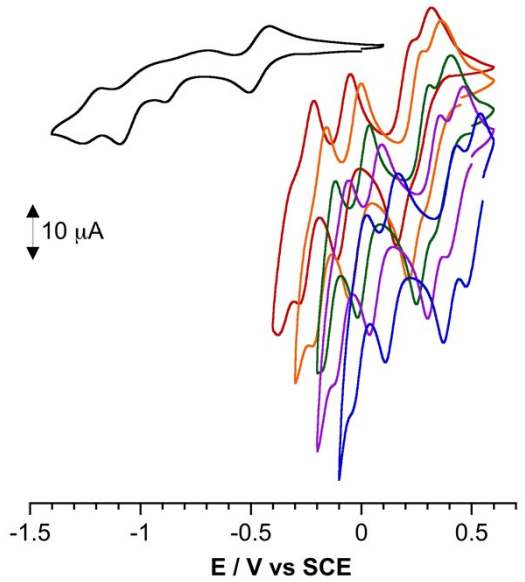

Figure S6. Cyclic voltammograms of **K^{Mo}_{Sn}[I]** (black curve, scan rate 20 mV s^{-1}) 1 mM in MeCN containing 0.1 M $TBAPF_6$ solutions and after the addition of 30 (red), 60 (orange), 100 (green), 200 (purple) and 500 (blue) equiv. of trifluoroacetic acid (TFA); working electrode, glassy carbon; reference electrode, SCE.

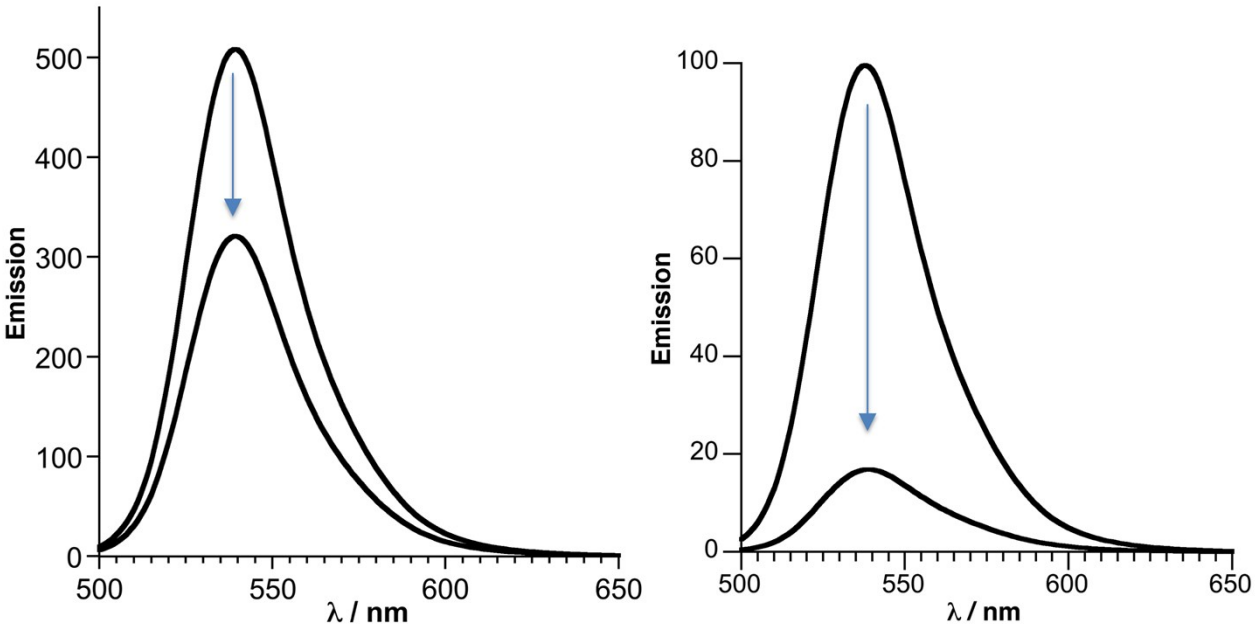

Figure S7. Evolution of the emission spectra of **K^{W}_{Sn}[BOD]** (left) and **K^{Mo}_{Sn}[BOD]** (right) upon the addition of 500 equiv. TFA.

Table S1. Quantum yield of the POM-bod hybrid and BOD-TMS in MeCN recorded against Rhodamine 6G in MeOH as a reference).

	ϕ
BOD-TMS	0.43
K^{W}_{Sn}[BOD]	0.40
K^{W}_{Sn}[BOD] + 500 equiv. TFA	0.25
K^{Mo}_{Sn}[BOD]	0.19
K^{Mo}_{Sn}[BOD] + 500 equiv. TFA	0.03

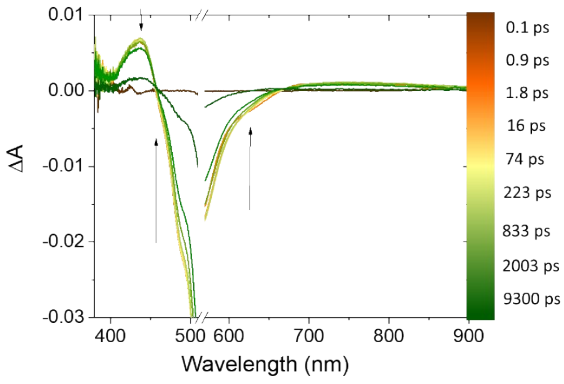

Figure S8. fs-resolution transient absorption spectra of **BOD** in MeCN following excitation at 540 nm, τ = 5.1 ns.

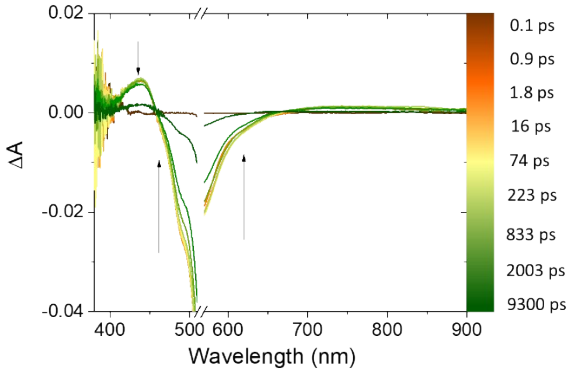

Figure S9. fs-resolution transient absorption spectra of **BOD** in MeCN + 500 equiv. TFA following excitation at 540 nm, τ = 5.1 ns.

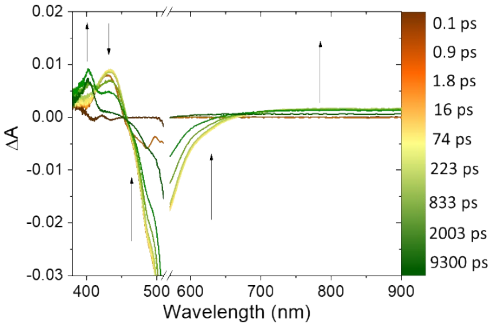

Figure S10. fs-resolution transient absorption spectra of $\mathbf{K^{W}_{Sn}[BOD]}$ in MeCN + 30 equiv. TFA following excitation at 540 nm.

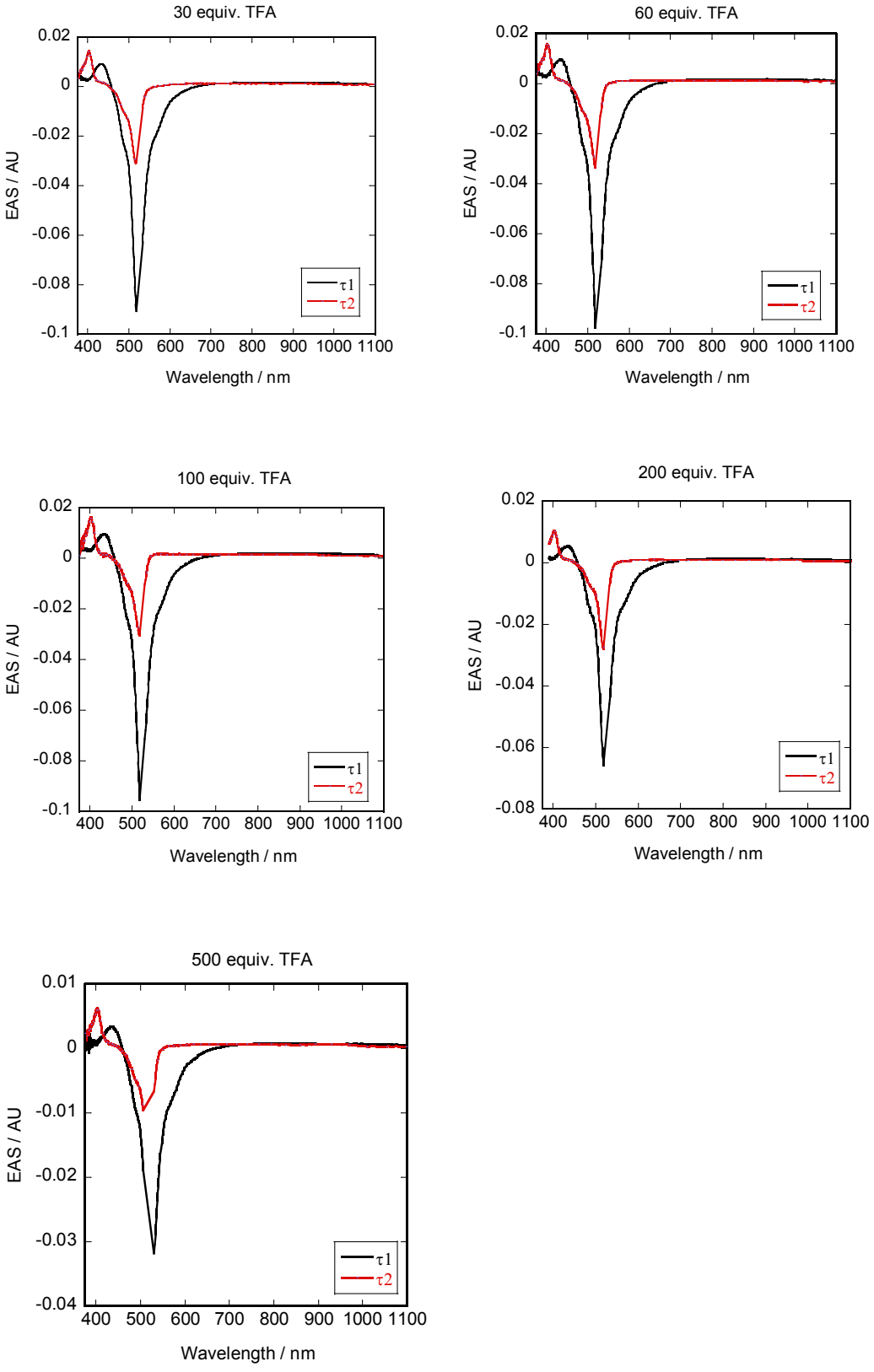

Figure S11. Evolution associated spectra on the addition of [H⁺] from fitting the fs-resolution transient absorption spectroscopy of $\mathbf{K^{W}_{Sn}[BOD]}$ in MeCN following excitation at 540 nm.

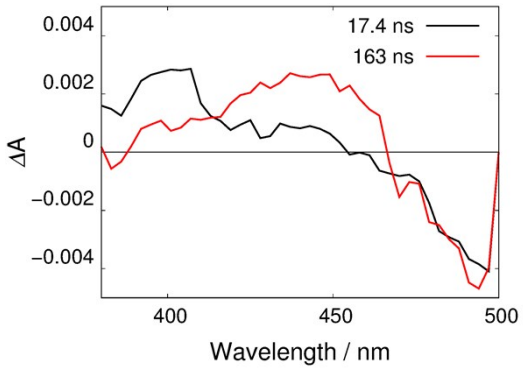

Figure S12. Nanosecond flash photolysis traces for **K$^{W}_{Sn}$[BOD]** in MeCN + 30 equivalents of TFA and excited at 540 nm, showing the charge separated state evolves into the triplet (red trace, multiplied by 10 × for clarity).

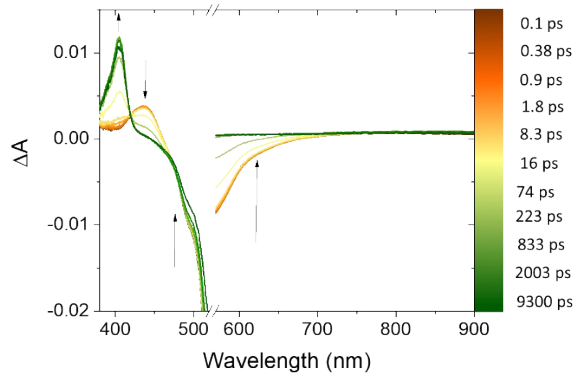

Figure S13: fs-resolution transient absorption spectra of **K$^{Mo}_{Sn}$[BOD]** in MeCN + 30 equiv. TFA following excitation at 540 nm.

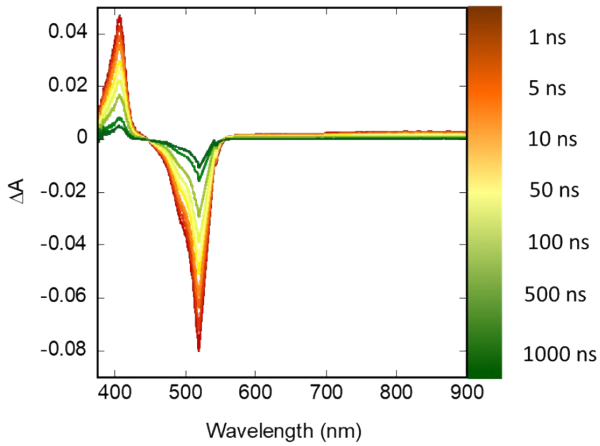

Figure S14: ns-resolution transient absorption spectra of **K$^{Mo}_{Sn}$[BOD]** in MeCN + 30 equiv. TFA following excitation at 532 nm.

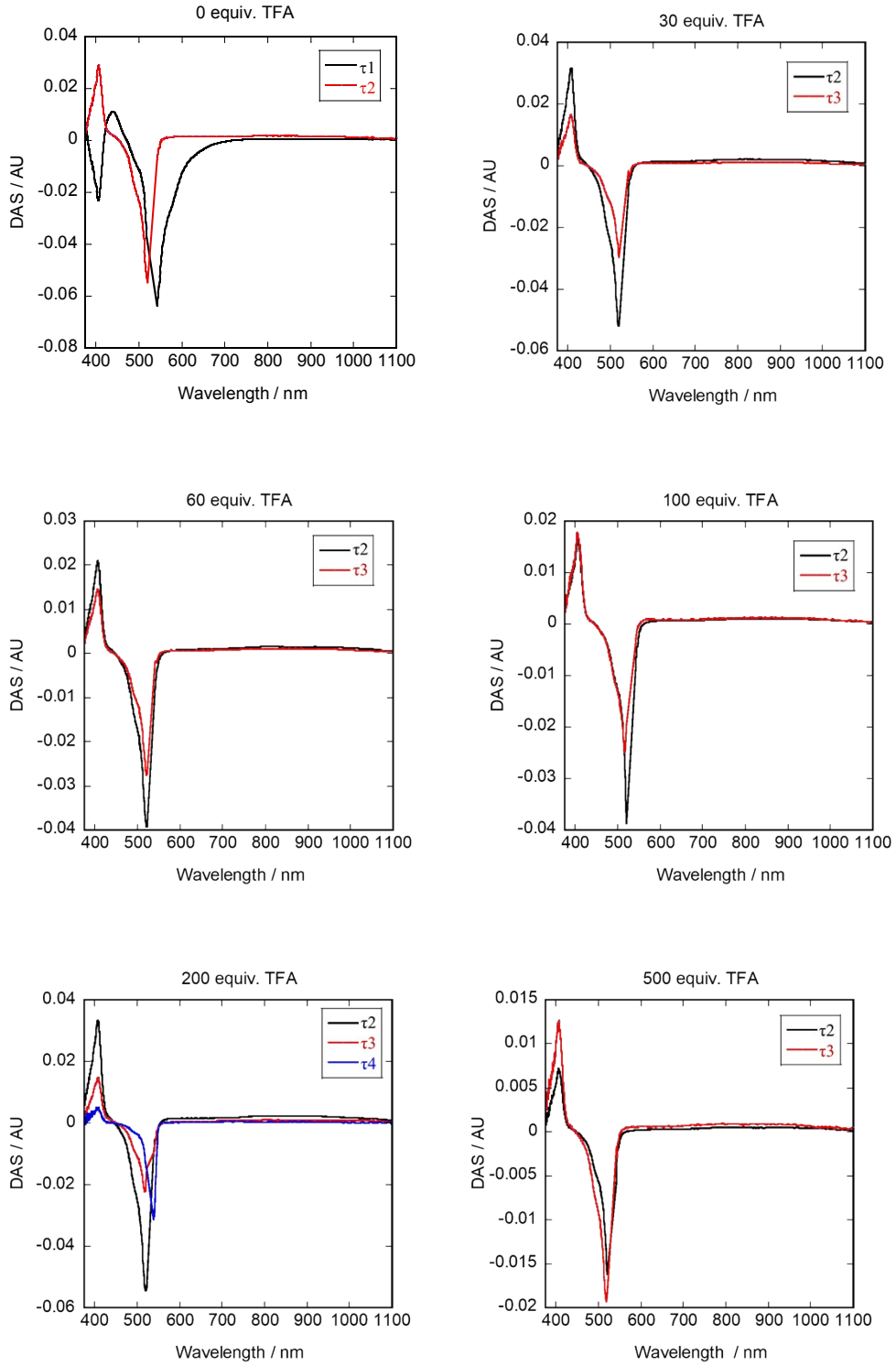

Figure S15. Decay associated spectra on the addition of [H^+] from fitting the ns-resolution flash photolysis **K^{Mo}_{Sn}[BOD]** in MeCN following excitation at 540 nm. τ_4 for 200 equiv. TFA is a minor component required to fit the data an is mostly due to scattering from the pump beam.

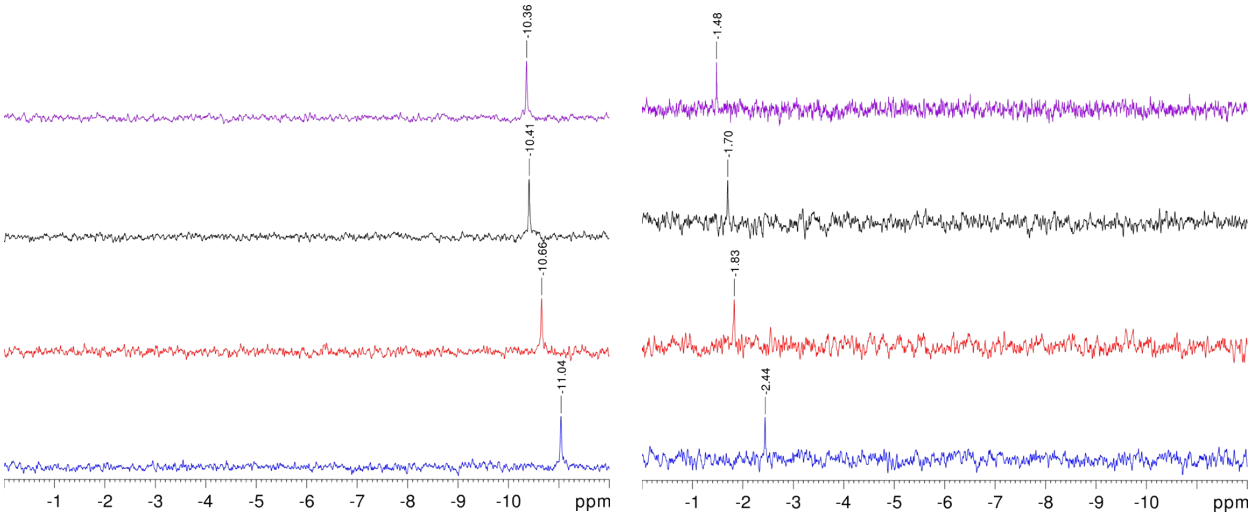

Figure S16. ^{31}P NMR spectra of solutions of **K^{W}_{Sn}[BOD]** (left) or **K^{Mo}_{Sn}[BOD]** (right) in CD_3CN containing increasing amounts of TFA (Blue: 0 eq TFA, red 30 eq, black 100 eq, purple 200 eq.).

Table S2. Global analysis fitting for fs-resolution transient absorption spectrum **K^{W}_{Sn}[BOD]** in MeCN with additions of TFA. τ_1 corresponds to the excited state, τ_2 corresponds to the charge-separated state. *The last delay is 10 ns so there is considerable error in τ_2.

Equiv. TFA	τ_1 (ns)	*τ_2 (ns)**
0	4.1	-
30	2.28	*10.6*
60	2.39	*10.3*
100	2.42	*8.40*
200	2.59	*11.6*
500	2.73	*7.2*

Table S3. Global analysis fitting for ns-resolution flash photolysis **K^{W}_{Sn}[BOD]** in MeCN with additions of TFA. τ_1 corresponds to the excited state, τ_2 is the charge-separated state at ca. 405 nm, τ_3 corresponds to the triplet state at ca. 450 nm. * NB τ_3 is an estimate because the time base of the experiment was set to 50 ns in order to capture τ_2. The pulse width in this experiment is 4 ns so it was not possible to extract τ_1.

Equiv. TFA	*τ_1 (ns)*	τ_2 (ns)	*τ_3 (ns)**
0	*6.3*	-	*200*
30	-	8.3	*300*
60	-	9	*250*
90	-	9.5	*250*
100	-	11	*2800*
200	-	30	*100000*
500	-	36	*long*

Table S4. Global analysis fitting for **K^{Mo}_{Sn}[BOD]** in MeCN with additions of TFA in the fs regime. **τ_1** corresponds to the excited state, **τ_2** corresponds to the charge-separated state. *NB the longest delay was 10 ns, so **τ_2** is not meaningful.

Equiv. TFA	τ_1 (ps)	τ_2* (ns)
0	2200	*30*
30	184	*35*
60	139	*45*
100	100	*330*
200	84	*82*
500	91	*75*

Table S5. Global analysis of ns-resolution flash photolysis for **K^{Mo}_{Sn}[BOD]** in MeCN with additions of TFA. **$\tau_{2\text{-}3}$** correspond to the charge-separated state.

Equiv. TFA	τ_1 (ns)	τ_2(ns)	%	τ_3 (ns)	%	τ_4 (ns)	%
0	2.1	16	-	-	-	-	-
30	-	32	66	885	34	-	-
60	-	31	59	922	41	-	-
100	-	32	48	980	52	-	-
200	-	32	63	1023	28	190000	9
500	-	28	38	1300	62	-	-

References

1. G. Ulrich and R. Ziessel, Convenient and efficient synthesis of functionalized oligopyridine ligands bearing accessory pyrromethene-BF2 fluorophores, *J. Org. Chem.*, 2004, **69**, 2070-2083.
2. B. Matt, J. Moussa, L. M. Chamoreau, C. Afonso, A. Proust, H. Amouri and G. Izzet, Elegant Approach to the Synthesis of a Unique Heteroleptic Cyclometalated Iridium(III)-Polyoxometalate Conjugate, *Organometallics*, 2012, **31**, 35-38.
3. C. Rinfray, S. Renaudineau, G. Izzet and A. Proust, A covalent polyoxomolybdate-based hybrid with remarkable electron reservoir properties, *Chem. Commun.*, 2014, **50**, 8575-8577.
4. O. Dangles, F. Guibe, G. Balavoine, S. Lavielle and A. Marquet, Selective Cleavage of the Allyl and Allyloxcarbonyl Groups through Palladium-Catalyzed Hydrostannolysis with Tributyltin Hydride - Application to the Selective Protection-Deprotection of Amino-Acid Derivatives and in Peptide-Synthesis, *J. Org. Chem.*, 1987, **52**, 4984-4993.